Journal of Engineering Mathematics Vol.II, No.2, April 1968.
Wolters-Noordhoff Publishing - Groningen
Printed in the Netherlands.

LIFT AND DRAG CHARACTERISTICS OF A DELTA-WING-HALF-CONE CONFIGURATION WITH SUBSONIC LEADING EDGES, USING SLENDER-BODY THEORY

W. J. Bannink and J. W. Reyn

Technological University Delft, the Netherlands

SUMMARY

Configurations, composed of a cone with a half-circular cross-section mounted above or below a delta wing of zero thickness with subsonic leading edges and placed in a supersonic flow, are studied using the slender-body theory in order to determine their lift and drag characteristics. These are compared to the lift and drag of configurations composed of the same wing and a symmetrically disposed circular cone with equal volume as the half-cone. The comparison is made to investigate whether it is possible to attain better lift efficiency by placing the body on one side of the wing.

For configurations having a body diameter-wing span ratio larger than approximately 0.45, a disposition of a half-cone on one side of the delta wing shows a drag reduction at a given lift, and therefore a higher value of $(C_L/C_D)_{max}$, compared to the corresponding symmetrical combination. However, the high-wing combination is preferable to the low-wing, since lower angles of incidence are needed to attain a certain C_L.

If the body diameter-wing span ratio is less than this value, the symmetrical system appears to be more favourable.

The lift curve slope $\frac{dC_L}{d\alpha}$ of the asymmetrical configurations studied is larger than that of the symmetrical configurations.

1. *Introduction.*

In order to improve theoretically possible lift and drag characteristics of supersonic aircraft various investigations have been made (for example see [1], [2], [3]).

For the major part these approaches concerned an arrangement of wing and body such that a favourable pressure interference effect could be obtained, to increase lift and to decrease drag. For wing-body combinations having wings with sonic or supersonic edges, a disposition with a body underneath the wing appeared to be an efficient means of generating lift [2], [3].

Also it is possible to reduce the drag at a given lift by indentations of the fuselage at the wing station, as has been investigated by Ferri e.a. [2], using the linear theory.

Any possibility of generating lift has to be considered together with the contingent drag that may result from it.

This finds expression in the lift-drag ratio, L/D. Using the linear theory Ferri e.a. [2] showed that in the case of a delta wing with supersonic leading edges the L/D ratio may increase when mounting a suitably selected double wedge underneath. The drag of the modified system appeared to be lower than that of the delta wing alone at the same lift. In addition, mounting the wedge means adding volume. An extension of this idea has been investigated, making use of the linear theory, by Reyn and Clarke [3], who considered an analogous configuration with a half-cone instead of a wedge and who also gave attention to arrowhead wings. In their case the wing leading edges were sonic. Reyn and Clarke compared the lift and drag characteristics of various configurations, namely a high-wing and a low-wing both carrying a half-cone, and a mid-wing with a full cone of the

same volume as the half-cone. The maximum drag reduction found in [3] for a high arrowhead wing-cone configuration appeared to be 37% and 10% as compared to the low-wing and mid-wing configurations, respectively. In the case of the delta wing these percentages were 15% and 2%. The results mentioned above may be expected, considering the fact that a body underneath the wing will induce a positive pressure on its own surface and on the undersurface of the wing. This results in a positive lift. The change of the body by bringing the whole volume to one side of the wing however, introduces an additional drag which may be considered as payment for the lift increase. In the case studied in [2] and [3] a favourable effect on the L/D ratio of a wing carrying a body underneath was found.

The question arises, whether such effect also remains present for wing-body configurations having subsonic leading edges. Then the overpressure at the undersurface of the wing "leaks" around the leading edges, thereby weakening the lift effect of the fuselage.

In the present paper the slender-body theory of Ward [4] is applied to wing-body configurations consisting of a delta wing with a half-cone mounted centrally underneath or above. The lift and drag characteristics are then compared to those of the mid-wing configuration, with a full cone having the same volume as the half-cone. An attached flow model is assumed. The paper is an abstract of [7], to which is referred to for further details.

After [7] had been written, the work of Portnoy [5], where the flow past a delta wing-half-cone combination with subsonic leading edges was investigated using the linear theory, came to the attention of the authors. Furthermore Portnoy treated the same problem in the framework of slender-body theory in an as yet unpublished paper [6].

Since the latter followed a different treatment of the problem then used in the present paper, yet obtained identical numerical results regarding the lift-drag characteristics, both approaches may serve as independent checks on the calculations. Moreover the present paper gives the comparison of the various wing-cone configurations.

2. *Statement of the problem.*

A sketch of the configuration consisting of a delta wing and a half-cone to be studied is given in fig.1, where also the body axes x, y, z are

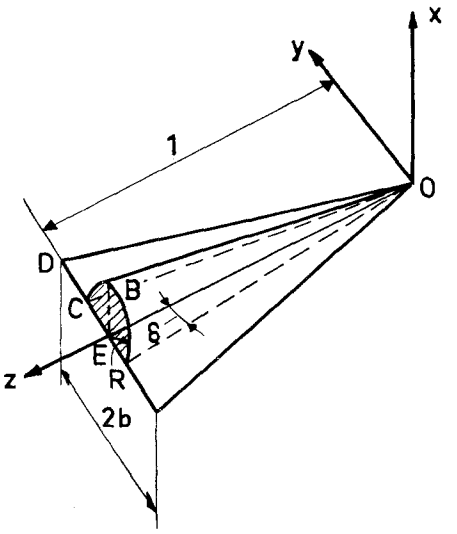

Fig.1: Sketch of the wing-body configuration

indicated. The wing span at the base is 2b and the rootchord is 1; the cone of radius R(1) at the base, has a semi apex angle of δ. This configuration is placed in a uniform supersonic flow of velocity U. The velocity vector lies in the xz plane and forms an angle α with the z-axis, α being positive for a positive rotation about the y-axis. According to the slender-body theory of Ward [4] the perturbation potential is given with respect to the wind axes x_w, y_w, z_w having the same origin as the body axes and with Oz_w parallel to the undisturbed flow. The perturbation potential is found to be given by

$$\Phi(x_w, y_w; z_w) = g(z_w) + \varphi'(x_w, y_w; z_w) \tag{1}$$

where $g(z_w)$ is a given function of the cross-sectional area distribution $S(z_w)$ of the configuration, and of the Mach number M; $\varphi'(x_w, y_w; z_w)$ satisfies the Laplace equation in the plane z_w = constant with the boundary condition

$$\frac{\partial \varphi'}{\partial \nu_w} = U \frac{\partial \nu_w}{\partial z_w} \tag{2}$$

on the body contour, where ν_w is the outward normal on the contour in the plane z_w = constant.

In addition, at infinity $\varphi'(x_w, y_w; z_w)$ must behave like

$$\varphi'(x_w, y_w; z_w) = \frac{U}{2\pi} \frac{dS(z_w)}{dz_w} \log r_w \tag{3}$$

where $r_w = (x_w^2 + y_w^2)^{\frac{1}{2}}$

The determination of the flow field past the configuration now involves the solution of the Laplace equation, which fulfils the boundary condition on the body eq. (2) and the condition at infinity eq. (3).

The problem thus stated will be transposed on body axes and split up into two parts, the boundary conditions will be split up accordingly. We then have

I the problem due to the flow at zero incidence with the perturbation potential $\varphi_0'(x, y; z)$;

II the problem due to the cross-flow at incidence α with the perturbation potential $\varphi_\alpha(x, y; z)$.

The problems I and II will be solved in the cross-sectional plane z = constant, called the ζ-plane given in fig. 2, where

$$\zeta = x + iy \tag{4}$$

Problem I ($\alpha = 0$)

In this case the body axes and wind axes coincide.

For the boundary condition on the wing we take

$$\frac{\partial \varphi_0'}{\partial x} = 0 \tag{5a}$$

and on the body

$$\frac{\partial \varphi_0'}{\partial r} = U \frac{dR(z)}{dz}, \quad \text{for } |\zeta| = R, \ 0 < \theta < \frac{\pi}{2} \tag{5b}$$

where θ represents the polar angle.
At infinity we shall require

$$\lim_{r\to\infty}\left[\varphi'_0 - \frac{U}{2\pi}\frac{dS(z)}{dz}\log r\right] = 0 \tag{6}$$

where $r = (x^2+y^2)^{\frac{1}{2}}$.

Problem II ($\alpha \neq 0$)

In this problem we take the boundary conditions on the wing surface

$$\frac{\partial\varphi_\alpha}{\partial x} = -U\alpha \tag{7a}$$

and on the body

$$\frac{\partial\varphi_\alpha}{\partial r} = -U\alpha\cos\theta, \tag{7b}$$

whereas at infinity we take

$$\varphi_\alpha = 0 \tag{8}$$

Superposition of the perturbation potentials φ'_0 and φ_α, satisfying the stated boundary conditions, yields the solution of the potential $\varphi'(x_w, y_w; z_w)$ for the boundary conditions eqs. (2) and (3).

3. *Conformal transformation of the ζ-plane.*

To solve the stated problems, the ζ-plane (fig. 2) is mapped onto the

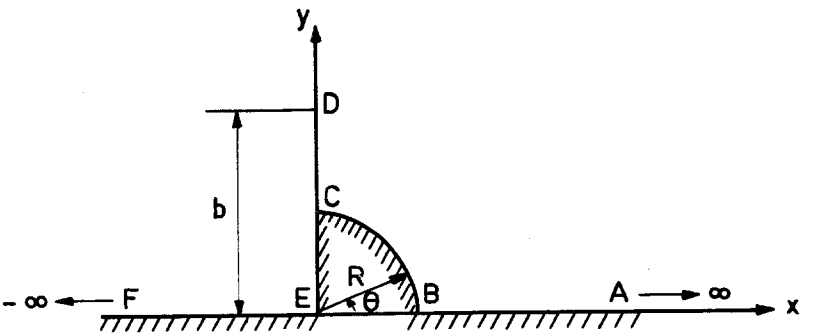

Fig. 2: The ζ-plane

τ-plane.
Since the configuration is symmetrical with respect to the xz-plane, only one half will be considered.
First we transform to a η-plane (fig. 3) by

$$\eta = \log\frac{\zeta}{R} \tag{9}$$

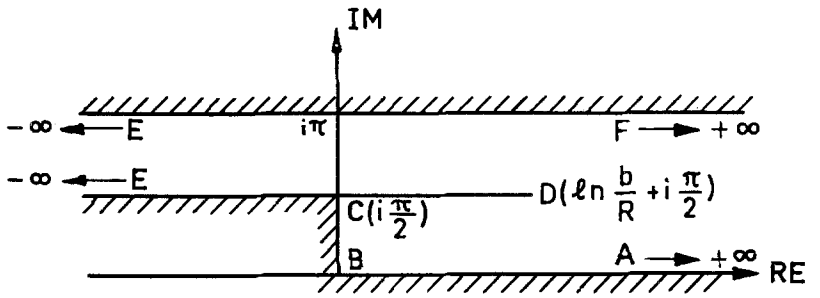

Fig. 3: The η-plane

The contour in the η-plane is a polygon, which may be transformed by a a Schwarz-Christoffel transformation onto the real axis of the τ-plane, see fig. 4 Choosing B in $\tau = \beta$, C in $\tau = 1$, D in $\tau = \lambda$ and E in $\tau = 0$ we

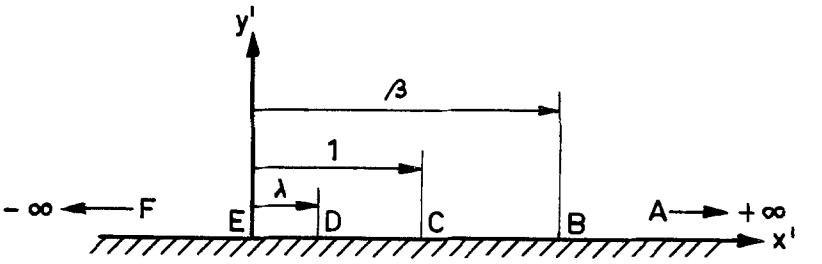

Fig. 4: The τ-plane

obtain with the Schwarz-Christoffel equation a conformal mapping of the inner region of the contour in the η-plane onto the upper half τ-plane [7].

The transformation formula is given by

$$\eta = \log\left[(\tau-\beta)^{\frac{1}{2}}+(\tau-1)^{\frac{1}{2}}\right]^2 + \log\left[\frac{-(\tau-\beta)^{\frac{1}{2}}+\left\{\beta(\tau-1)\right\}^{\frac{1}{2}}}{\tau^{\frac{1}{2}}}\right] - \frac{3}{2}\log(\beta-1) \quad (10)$$

whereas for λ follows $\lambda = \frac{1}{2}\beta^{\frac{1}{2}}$.

From eq. (10) the equation mapping the ζ-plane onto the τ-plane is found to be

$$\frac{\zeta}{R} = -(\beta-1)^{-\frac{3}{2}}\left[(\tau-\beta)^{\frac{1}{2}}+(\tau-1)^{\frac{1}{2}}\right]^2\left[\frac{(\tau-\beta)^{\frac{1}{2}}-\left\{\beta(\tau-1)\right\}^{\frac{1}{2}}}{\tau^{\frac{1}{2}}}\right] \quad (11)$$

where β is given by

$$\frac{b}{R} = \frac{\left[(\beta-\frac{1}{2}\beta^{\frac{1}{2}})^{\frac{1}{2}}+(1-\frac{1}{2}\beta^{\frac{1}{2}})^{\frac{1}{2}}\right]^2\left[(\beta-\frac{1}{2}\beta^{\frac{1}{2}})^{\frac{1}{2}}-\left\{\beta(1-\frac{1}{2}\beta^{\frac{1}{2}})\right\}^{\frac{1}{2}}\right]}{\left[\frac{1}{2}(\beta-1)^3\beta^{\frac{1}{2}}\right]^{\frac{1}{2}}} \quad (12)$$

Eq. (12) gives the relation between the body diameter-wing span ratio and β. As a check, eq. (11) may be applied to the case of the wing alone. Then in the limit the points B and C of fig. 2 coincide in $\zeta = 0$, and eq. (11) passes into

$$\frac{\zeta}{b} = 2\left[\tau(\tau-1)\right]^{\frac{1}{2}} \tag{13}$$

The behaviour at infinity of eq. (11) is of importance in the solution of boundary value-problem I. For $\zeta \to \infty$ eq. (11) becomes

$$\frac{\zeta}{R} = \frac{4(\beta^{\frac{1}{2}}-1)}{(\beta-1)^{\frac{3}{2}}}\tau \tag{14}$$

4. Solution of problem I ($\alpha = 0$).

Firstly we satisfy the boundary conditions eq. (5a) and eq. (5b) by placing a source distribution on the contour of the body. Fig. 5 shows a sketch of

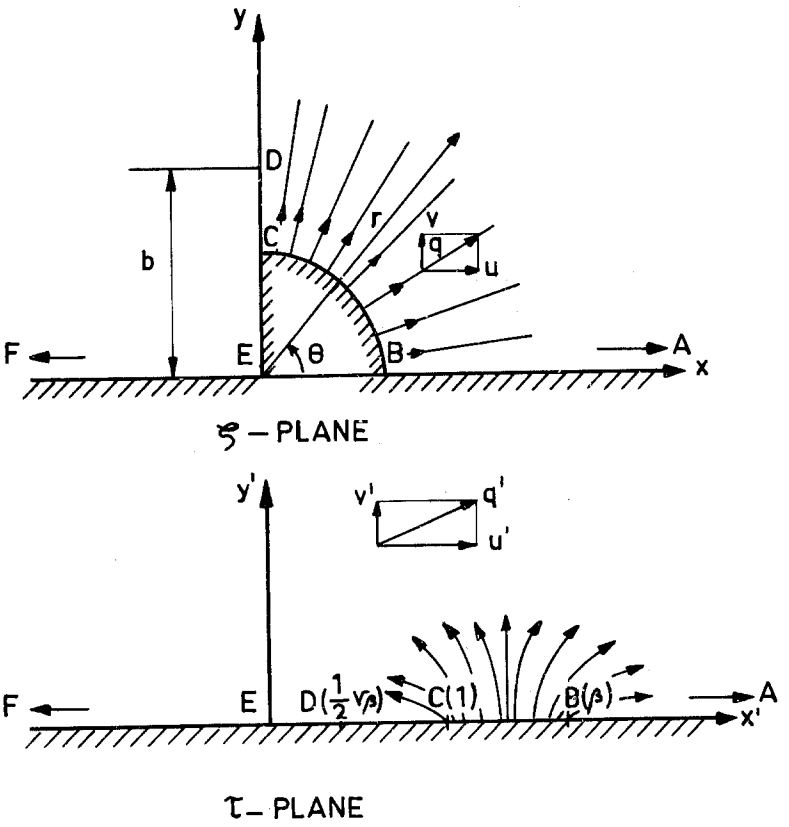

Fig. 5: Flow in a cross-section z = c = const. Problem I ($\alpha = 0$)

the flow pattern in the ζ-plane and the corresponding τ-plane. The body contour corresponds to $1 < x' < \beta$, $y' = 0$ in the τ-plane, where

$$\tau = x' + iy' \tag{15}$$

If

$$\chi_0 = \varphi_0(x', y') + i\psi_0(x', y') = \varphi_0(x, y) + i\psi_0(x, y) \tag{15a}$$

is the complex potential, we may write

$$\frac{\partial \varphi_0}{\partial r} = \frac{\partial \varphi_0}{\partial x'}\frac{\partial x'}{\partial r} + \frac{\partial \varphi_0}{\partial y'}\frac{\partial y'}{\partial r}, \tag{16}$$

where r, θ are polar coordinates in the ζ-plane (see fig. 5).

With $\frac{\partial x'}{\partial r} = 0, \frac{\partial y'}{\partial r} = \left|\frac{d\tau}{d\zeta}\right|$ and eqs (5b) and (11) there follows from eq. (16) for the boundary conditions on the body in the τ-plane

$$\frac{\partial \varphi_0}{\partial y'}(x', 0) = U R \frac{dR}{dz} \frac{x' - \frac{1}{2}\beta^{\frac{1}{2}}}{x'(x'-1)^{\frac{1}{2}}(\beta - x')^{\frac{1}{2}}} \tag{17a}$$

Elsewhere on the real x'-axis is

$$\frac{\partial \varphi_0}{\partial y'}(x', 0) = 0 \tag{17b}$$

The conditions (17a) and (17b) are satisfied by a source distribution of strength

$$\frac{U}{\pi} R \frac{dR}{dz} \frac{x' - \frac{1}{2}\beta^{\frac{1}{2}}}{x'(x'-1)^{\frac{1}{2}}(\beta - x')^{\frac{1}{2}}} \tag{17c}$$

on the real axis of the τ-plane for $1 < x' < \beta$.

The potential in the τ-plane then becomes

$$\varphi_0(x', y') = \frac{U}{\pi} R \frac{dR}{dz} \int_1^\beta \frac{\xi - \frac{1}{2}\beta^{\frac{1}{2}}}{\xi(\xi-1)^{\frac{1}{2}}(\beta - \xi)^{\frac{1}{2}}} \log\left[(x'-\xi)^2 + y'^2\right]^{\frac{1}{2}} d\xi \tag{18}$$

and the velocities

$$\frac{\partial \varphi_0}{\partial x'}(x', y') = \frac{U}{\pi} R \frac{dR}{dz} \int_1^\beta \frac{\xi - \frac{1}{2}\beta^{\frac{1}{2}}}{\xi(\xi-1)^{\frac{1}{2}}(\beta - \xi)^{\frac{1}{2}}} \frac{|x' - \xi|}{(x'-\xi)^2 + y'^2} d\xi \tag{19}$$

and

$$\frac{\partial \varphi_0}{\partial y'}(x', y') = \frac{U}{\pi} R \frac{dR}{dz} \int_1^\beta \frac{\xi - \frac{1}{2}\beta^{\frac{1}{2}}}{\xi(\xi-1)^{\frac{1}{2}}(\beta - \xi)^{\frac{1}{2}}} \frac{y'}{(x'-\xi)^2 + y'^2} d\xi \tag{20}$$

For the calculation of the lift and drag with the slender-body theory we only need the potential and the normal velocity on the contour of the configuration. The evaluation of the integrals (18) and (19) has been carried out in detail in [7]. In the present paper only the final results will be given. We then find
for $x' < 1$

$$\varphi_0(x', 0) = 2\, U R \frac{dR}{dz}\left[\log \frac{(\beta - x')^{\frac{1}{2}} + (1 - x')^{\frac{1}{2}}}{2} - \frac{1}{2}\log \frac{(\beta - x')^{\frac{1}{2}} + \left\{\beta(1-x')\right\}^{\frac{1}{2}}}{\beta^{\frac{1}{2}} + 1}\right], \tag{21}$$

$$\frac{\partial \varphi_0}{\partial x'}(x', 0) = -\, U R \frac{dR}{dz}\frac{1}{x'}\left[\frac{x' - \frac{1}{2}\beta^{\frac{1}{2}}}{(\beta - x')^{\frac{1}{2}}(1-x')^{\frac{1}{2}}} + \frac{1}{2}\right]; \tag{22}$$

for $1 < x' < \beta$

$$\varphi_0(x',0) = U R \frac{dR}{dz}\left[\log\frac{(\beta-1)^{\frac{1}{2}}(\beta^{\frac{1}{2}}+1)}{4} - \tfrac{1}{2}\log x'\right], \tag{23}$$

$$\frac{\partial\varphi_0}{\partial x'}(x',0) = -\tfrac{1}{2} U R \frac{dR}{dz}\frac{1}{x'}; \tag{24}$$

and for $x' > \beta$

$$\varphi_0(x',0) = 2 U R \frac{dR}{dz}\left[\log\frac{(x'-\beta)^{\frac{1}{2}}+(x'-1)^{\frac{1}{2}}}{2} - \tfrac{1}{2}\log\frac{(x'-\beta)^{\frac{1}{2}}+\left\{\beta(x'-1)\right\}^{\frac{1}{2}}}{\beta^{\frac{1}{2}}+1}\right] \tag{25}$$

$$\frac{\partial\varphi_0}{\partial x'}(x',0) = U R \frac{dR}{dz}\frac{1}{x'}\left[\frac{x'-\frac{1}{2}\beta^{\frac{1}{2}}}{(x'-1)^{\frac{1}{2}}(x'-\beta)^{\frac{1}{2}}} - \tfrac{1}{2}\right] \tag{26}$$

So far the potential and the velocities have been determined using the boundary conditions on the configuration only.

Now we will check whether the condition at infinity given by eq. (6) is satisfied.

The behaviour at infinity of the potential may be found from eq. (21) for $x' < 1$ or from eq. (25) for $x' > \beta$. Using eq. (14) we find from eq. (21) for $x' \to -\infty$ from eq. (25) for $x' \to +\infty$

$$\varphi_0(x,y) = \frac{U}{2} R \frac{dR}{dz}\left[\log x - \log\frac{4(\beta^{\frac{1}{2}}-1)R}{(\beta-1)^{\frac{3}{2}}}\right] \tag{27}$$

If this result is compared with eq. (6) a relation between $\varphi_0(x,y)$ and $\varphi_0'(x,y)$ is obtained which is given by

$$\varphi_0'(x,y;z) = \varphi_0(x,y;z) + \frac{U}{2} R \frac{dR}{dz}\log\frac{4(\beta^{\frac{1}{2}}-1)R}{(\beta-1)^{\frac{3}{2}}} \tag{28}$$

The additional term dependent on z only does not alter the boundary condition on the contour of the configuration.

5. *Solution of problem II* ($\alpha \neq 0$).

In order to solve this problem we add a uniform cross-flow with velocity $U\alpha$ parallel to the x-axis, by introducing the function $\Phi_\alpha(x,y)$ defined by

$$\Phi_\alpha(x,y) = U\alpha x + \varphi_\alpha(x,y) \tag{29}$$

The boundary conditions given in eqs. (7a), (7b) and (8) are then trans-

formed to

$$\frac{\partial \Phi_\alpha}{\partial x} = 0 \tag{30a}$$

on the wing surface, and

$$\frac{a\Phi_\alpha}{\partial r} = 0 \tag{30b}$$

on the body.
At infinity we have

$$\Phi_\alpha = U\alpha x \tag{31}$$

By transforming the problem to the τ-plane, the boundary conditions are easily seen to be satisfied by a uniform flow parallel to the x'-axis. A sketch of the flow field in both planes is given in fig. 6.

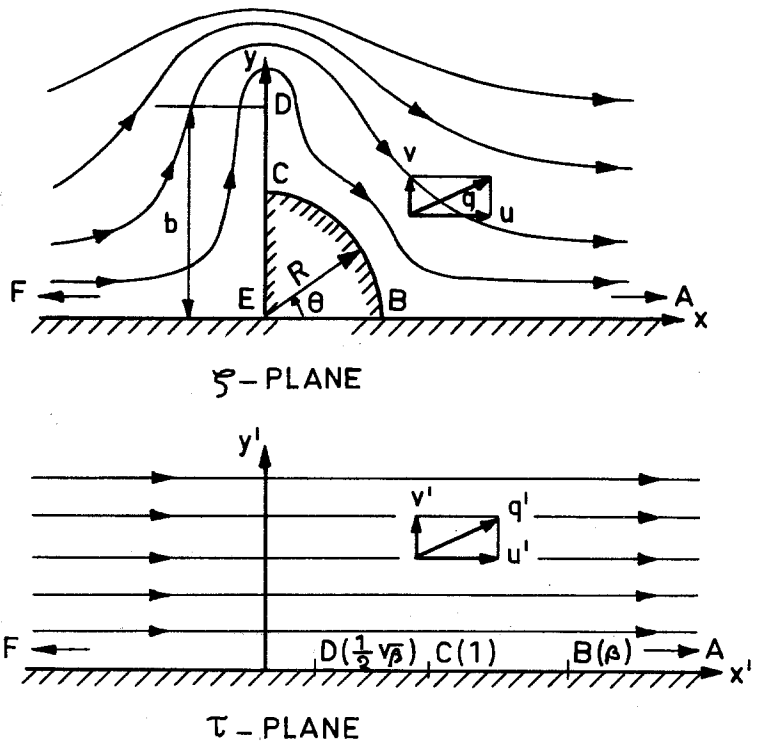

Fig. 6: Flow in a cross-section z = c = const. Problem II ($\alpha \neq 0$)

Let the complex potential be given by

$$\chi_\alpha(\tau) = \Phi_\alpha(x', y') + i\psi_\alpha(x', y') = a\tau \quad (a > 0) \tag{32}$$

then the conjugate velocity in the ζ-plane is found to be given by

$$\frac{d\chi_\alpha(\zeta)}{d\zeta} = \frac{d\chi_\alpha(\tau)}{d\tau}\,\frac{d\tau}{d\zeta} = a\,\frac{\tau(\zeta)\left\{\tau(\zeta)-1\right\}^{\frac{1}{2}}\left\{\tau(\zeta)-\beta\right\}^{\frac{1}{2}}}{\zeta\left\{\tau(\zeta)-\frac{1}{2}\beta^{\frac{1}{2}}\right\}} \tag{33}$$

The value of a is found from the condition at infinity eq. (31) and using eq. (14). Then follows

$$a = 4 R U \alpha \frac{\beta^{\frac{1}{2}} - 1}{(\beta - 1)^{3/2}} \tag{34}$$

The eqs. (32), (33) and (34) enable us to find the velocity-components on the contour of the configuration. This is done in [7]. For the calculation of the aerodynamic forces it suffices to know the real part Φ_α of the complex potential χ_α on the contour. The complex potential in the τ-plane follows from eqs. (32) and (34), giving

$$\chi_\alpha(\tau) = 4 R U \alpha \frac{\beta^{\frac{1}{2}} - 1}{(\beta - 1)^{\frac{3}{2}}} \tau \tag{35}$$

Hence, on the real axis of the τ-plane $\Phi_\alpha(x', y')$ becomes

$$\Phi_\alpha(x', 0) = 4 R U \alpha \frac{\beta^{\frac{1}{2}} - 1}{(\beta - 1)^{\frac{3}{2}}} x'. \tag{36}$$

6. *The aerodynamic forces.*

The solutions of problems I and II will now be used to calculate lift and drag of the delta wing-half-cone combination*. Lift and drag will be determined for each of the two problems separately, the total lift and drag then follow by superposition.

According to Ward [4] the lateral force on the combination is given by

$$\frac{F_{x_w} + i F_{y_w}}{\frac{1}{2} \rho U^2} = -\frac{2i}{U} \int_C \left[g(z_w) + \varphi'(x_w, y_w; z_w) \right]_{z_w = 1} d\zeta \tag{37}$$

where F_{x_w}, F_{y_w} are the components of the force in x_w, y_w direction, respectively and ρ is the density in the undisturbed flow ($\frac{1}{2}\rho U^2$ denotes the dynamic pressure).

The contour integral has to be taken around the contour C at the base $z_w = 1$. In the present case $F_{y_w} = 0$ and the component F_{x_w} represents the lift force L.

If we consider firstly the case where $\alpha = 0$ (then body axes and wind axes coincide), we obtain by substitution of eq. (28),

$$\frac{L_{\alpha = 0}}{\frac{1}{2} \rho U^2} = \frac{4}{U} \left[\tan\delta \int_0^{\pi/2} (\varphi_0)_{BC} \cos\theta \, d\theta + \int_{\tan\delta}^{b} (\varphi_0)_{CD} \, dy - \int_0^{b} (\varphi_0)_{DE} \, dy \right]_{z=1} \tag{38}$$

where δ is the semi-apex angle of the cone (for $z = 1$ is $\frac{dR}{dz} = R = \tan\delta$).

On the cone BC the potential $(\varphi_0)_{BC}$ is given by eq. (23) and from eq. (11) the relation between θ and x' is found to be

$$\cos\theta = \frac{1}{(\beta - 1)^{\frac{3}{2}}} \frac{(x' - 1)^{\frac{1}{2}}}{x'^{\frac{1}{2}}} \left[2(\beta - x') + (2x' - \beta - 1)\beta^{\frac{1}{2}} \right] \tag{39}$$

It may be remarked, that the solutions of problems I and II may also be used to calculate the lift and drag of wing-body combinations with curved leading edges, but having a wing span-body diameter ratio not varying in the flow direction.

On the wing CD and DE the potentials $(\varphi_0)_{CD}$, $(\varphi_0)_{DE}$ follow from eq. (21), so that the last two integrals of eq. (38) may be evaluated using eq. (11).

Next the lift due to an angle of incicence α may be found in the same way by substituting φ_α from eqs. (29) and (36) in eq. (37). We may then derive the lift curve slope

$$\frac{1}{\frac{1}{2}\rho U^2}\frac{dL}{d\alpha} = \frac{4}{\alpha U}\left[\tan\delta \int_0^{\pi/2} (\Phi_\alpha)_{BC} \cos\theta\, d\theta + \int_{\tan\delta}^{b} (\Phi_\alpha)_{CD}\, dy - \int_0^{b} (\Phi_\alpha)_{DE}\, dy\right]_{z=1} - \pi\tan^2\delta \tag{40}$$

The slender-body expression for the wave drag at zero incidence of the configuration is found from the equation for a general body with length 1 [4], thus giving

$$\frac{D_{\alpha=0}}{\frac{1}{2}\rho U^2} = -\frac{1}{2\pi}\int_0^1\int_0^1 S''(z)\,S''(t)\log|z-t|\,dz\,dt + \frac{1}{\pi}S'(1)\int_0^1 S''(z)\log(1-z)dz - \frac{1}{2\pi}\left\{S'(1)\right\}^2\log\frac{(M^2-1)^{\frac{1}{2}}}{2} - \frac{1}{U^2}\left[\int_C \varphi_0'\frac{\partial\varphi_0'}{\partial\nu}\,ds\right]_{z=1} \tag{41}$$

where s is the distance along the contour.

Evaluating the first two integrals in eq. (41), and making use of eqs. (5b) and (28), yields the wave drag for the configuration at zero incidence

$$\frac{D_{\alpha=0}}{\frac{1}{2}\rho U^2} = \frac{\pi}{2}\tan^4\delta\left[\log\frac{(\beta-1)^{\frac{3}{2}}}{2(M^2-1)^{\frac{1}{2}}(\beta^{\frac{1}{2}}-1)\tan\delta} - \frac{1}{2}\right] - \frac{2\tan^2\delta}{U}\left[\int_0^{\pi/2}(\varphi_0)_{BC}\,d\theta\right]_{z=1} \tag{42}$$

The integral in eq. (42) may be evaluated using eq. (23) for $(\varphi_0)_{BC}$ and eq. (39) to give

$$\frac{D_{\alpha=0}}{\frac{1}{2}\rho U^2} = \frac{\pi}{2}\tan^4\delta\left[\log\frac{(\beta-1)^{\frac{1}{2}}(\beta^{\frac{1}{2}}+1)^4}{8\beta(\beta^{\frac{1}{2}}-1)(M^2-1)^{\frac{1}{2}}\tan\delta} - \frac{1}{2}\right] \tag{43}$$

Let $C_L = L/\frac{1}{2}\rho U^2 A$, $C = D/\frac{1}{2}\rho U^2 A$, where A is the wing area, be the lift and drag coefficient, respectively, then according to the slender-body theory th following relation may be found [4]:

$$C_D = (C_D)_{C_L=0} + \frac{1}{2}\left\{\alpha - (\alpha)_{C_L=0}\right\}C_L \tag{44}$$

or, since C_L is a linear function of α, for the polar curve is obtained

$$C_D = (C_D)_{\alpha=0} + \frac{1}{2\frac{dC_L}{d\alpha}}\left\{C_L^2 - (C_L)^2_{\alpha=0}\right\} \tag{45}$$

7. *Comparison of the various configurations.*

The high-wing and low-wing configuration may be compared to the con-

figuration having a delta wing with a symmetrically disposed full one. A comparison will be made of the aerodynamic forces of configurations with equal body volume and equal wing area. Then the following relation exists between apex angle of the half-cone and that of the full cone

$$\tan^2\gamma = \tfrac{1}{2}\tan^2\delta \tag{46}$$

where γ is the semi apex angle of the full cone.

The lift and drag of the symmetrical configuration is obtained from [4]. Substituting eq. (46) there follows for the lift curve slope of the mid-wing combination

$$\frac{dC_L}{d\alpha} = 2\pi\tan\delta\,\frac{b}{\tan\delta}\left[1-\tfrac{1}{2}\left(\frac{\tan\delta}{b}\right)^2+\frac{1}{4}\left(\frac{\tan\delta}{b}\right)^4\right] \tag{47}$$

and for the wave drag coefficient at zero incidence

$$(C_D)_{\alpha=0} = \frac{\pi}{2}\tan^3\delta\,\frac{\tan\delta}{b}\left[\log\frac{2^{\frac{3}{2}}}{(M^2-1)^{\frac{1}{2}}\tan\delta}-\tfrac{1}{2}\right] \tag{48}$$

The expression for the polar curve is

$$C_D = (C_D)_{\alpha=0} + \frac{1}{2\dfrac{dC_L}{d\alpha}}\cdot C_L^2 \tag{49}$$

For the comparison the maximum value of C_L/C_D is of interest. From eq. (45) there follows

$$(C_L/C_D)_{max} = \frac{\tfrac{1}{2}\left(\dfrac{dC_L}{d\alpha}\right)^{\frac{1}{2}}}{\left[(C_D)_{\alpha=0}-\dfrac{(C_L)^2_{\alpha=0}}{2\dfrac{dC_L}{d\alpha}}\right]^{\frac{1}{2}}} \tag{50}$$

The value of C_L and C_D at which $(C_L/C_D)_{max}$ occurs are called the optimum values, $(C_L)_{opt.}$ and $(C_D)_{opt.}$

Eq. (45) shows that the polar curves of the low-wing and the high-wing systems coincide. In order to obtain a certain value of C_L however, the incidence needed for a high-wing combination is much lower than for the corresponding low-wing combination. Therefore the high-wing is more interesting. A qualitative sketch of the polar curves of the asymmetrical and symmetrical configurations is shown in fig. 7. The value of C_L whereby both systems have equal lift and drag (the intersection point of the polar curves) is called the critical value, $(C_L)_{crit.}$. This value follows by equating eqs. (45) and (49).

Since the effect of Mach number is equally present in $(C_D)_{\alpha=0}$ of both configurations, $(C_L)_{crit.}$ is independent of the Mach number.

8. *Numerical results.*

The computations of C_L and C_D were carried out on the TR-4 computer of the Technological University Delft.

The results are illustrated in figs 8 to 12.

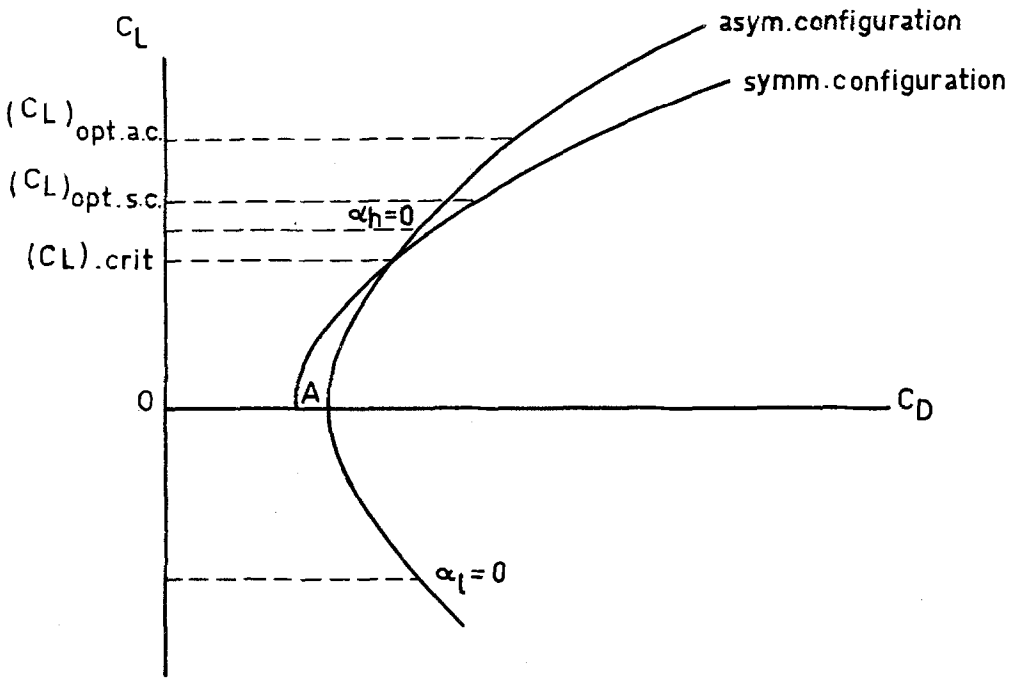

Fig. 7: Diagram of polar curves

Fig. 8 shows the value of C_L of the high-wing combination at zero incidence. Also shown is $(C_L)_{crit.}$; it is seen that the polar curves have an intersection point if $(\tan\delta/b) < 0.5$, thus for body diameters which are relatively small with respect to the wing span. For $(\tan\delta/b) > 0.5$, so for thicker bodies, the asymmetrical configuration shows at all value of C_L a lower value of C_D compared with the symmetrical system.

It appears that $\frac{dC_L}{d\alpha}$ of the asymmetrical configuration is higher than that of the corresponding symmetrical one. The ratio of the two is given as a function of the body diameter-wing span ratio in fig. 9.

Fig. 10 and 11 show C_L/C_D as a function of C_L for various apex angles of cone and delta wing and for M = 1.2 and 2.0.

At small values of $m = b(M^2 - 1)^{\frac{1}{2}}$ the ratio of the semi apex angle of the wing to the Mach angle is small. Then the slender-body theory is most accurate. At values of $(\tan\delta/b)$ below 0.47 the C_L/C_D of the symmetrical system is higher than that of the corresponding asymmetrical system, whereas the opposite occurs at values of $(\tan\delta/b)$ above 0.47. This means that if the cone angle is large compared to the delta wing apex angle the influence of placing the body on the lower side of the wing is favourable. The effect of the Mach number on the results is very small, as may be expected, since in the slender-body theory only C_D contains a weak dependence on the Mach number.

Rather then going into details about the values of C_L/C_D at arbitrary values of C_L, it might be interesting to compare the maximum values of C_L/C_D. It must be noted however, that $(C_L/C_D)_{max}$ of all types of configurations is attained at different values of C_L. If δ is taken smaller, $(C_L/C_D)_{max}$ appears at lower values of C_L (figs 10, 11). Also evident in figs. 10 and 11 is the fairly flat maximum in the curves at large values of δ as compared to the very small region of C_L where the highest values of C_L/C_D are reached to small cone angles. In the case of the high-wing system $(C_L/C_D)_{max}$ appears at an angle of incidence close to zero.

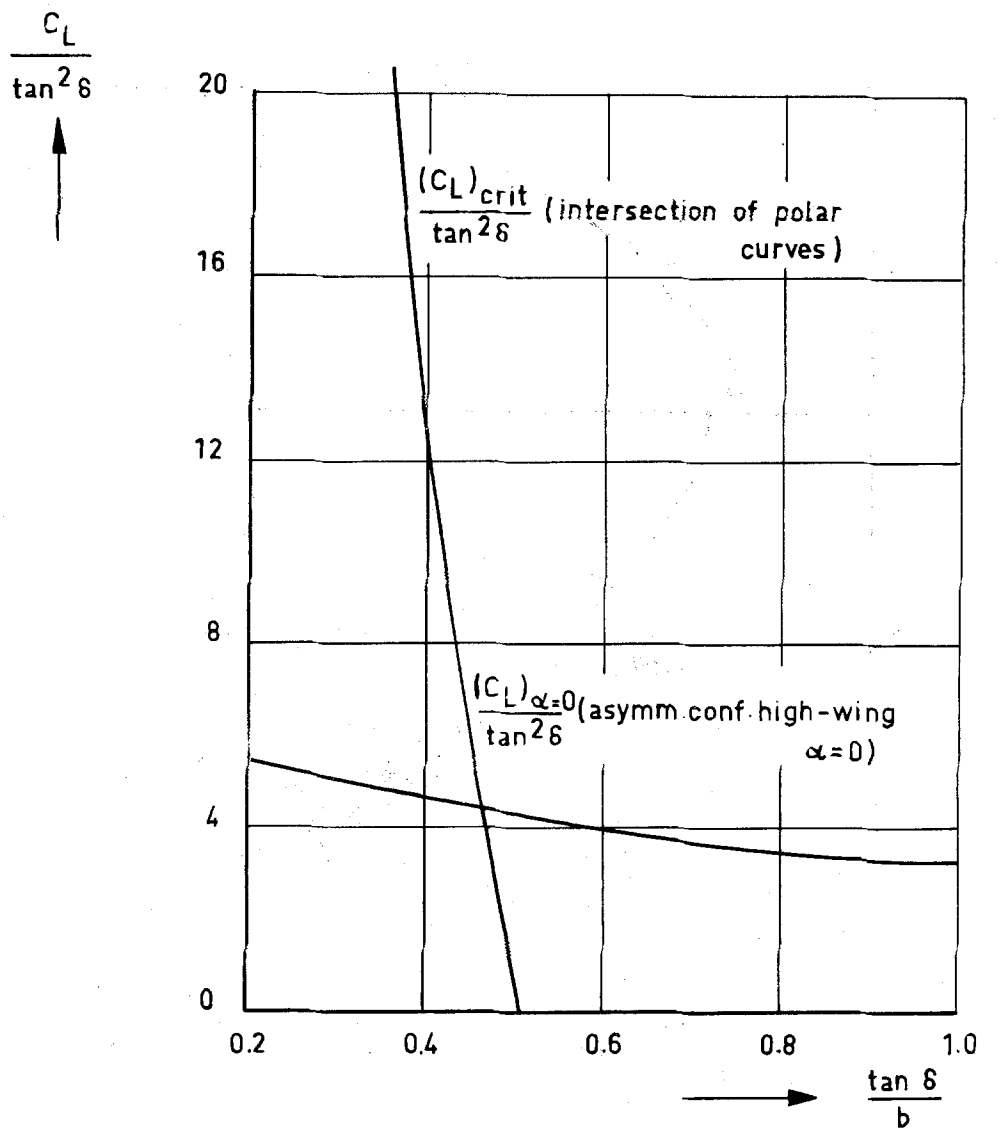

Fig. 8: $(C_L)_{crit}$ and $(C_L)_{\alpha=0}$ as a function of diameter - span ratio $\frac{\tan\delta}{b}$

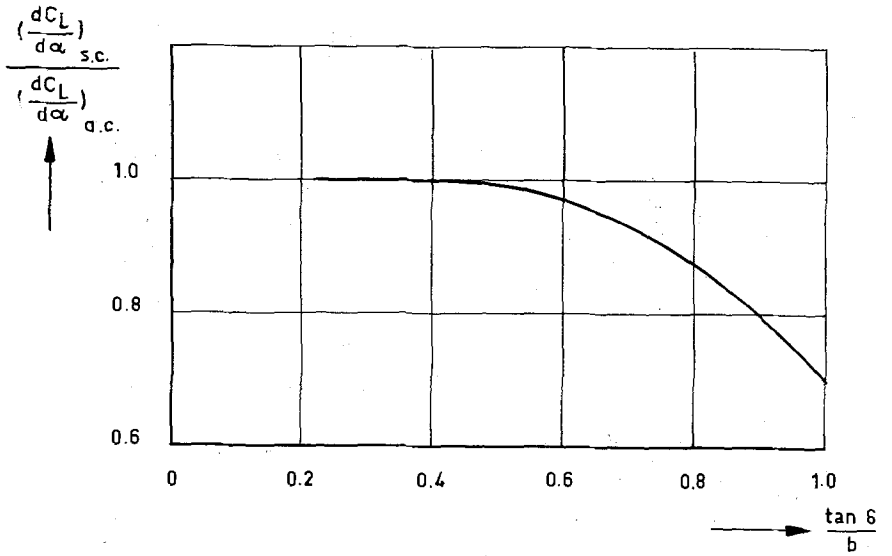

Fig. 9: Comparison between lift curve slopes of the symm. and asymm. configurations

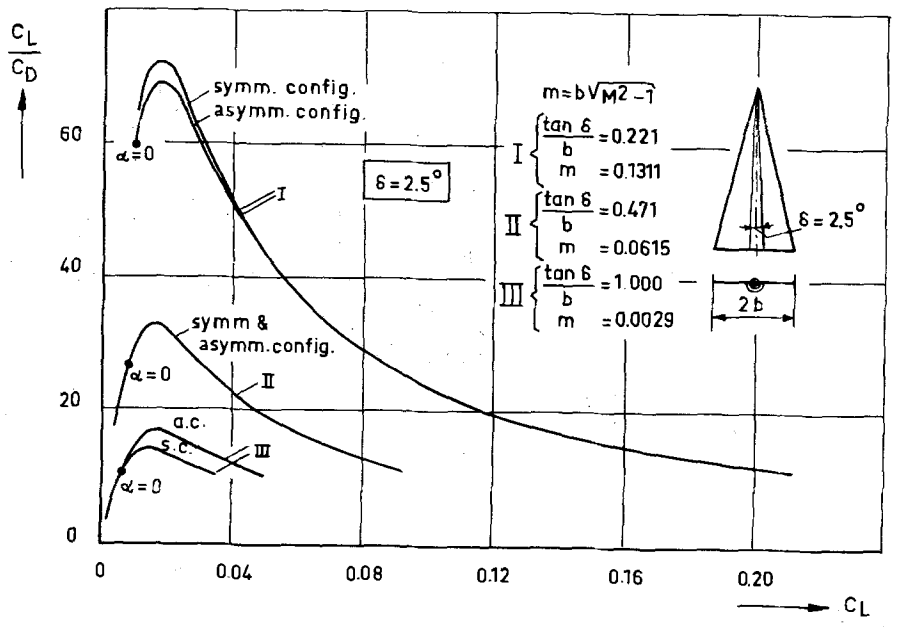

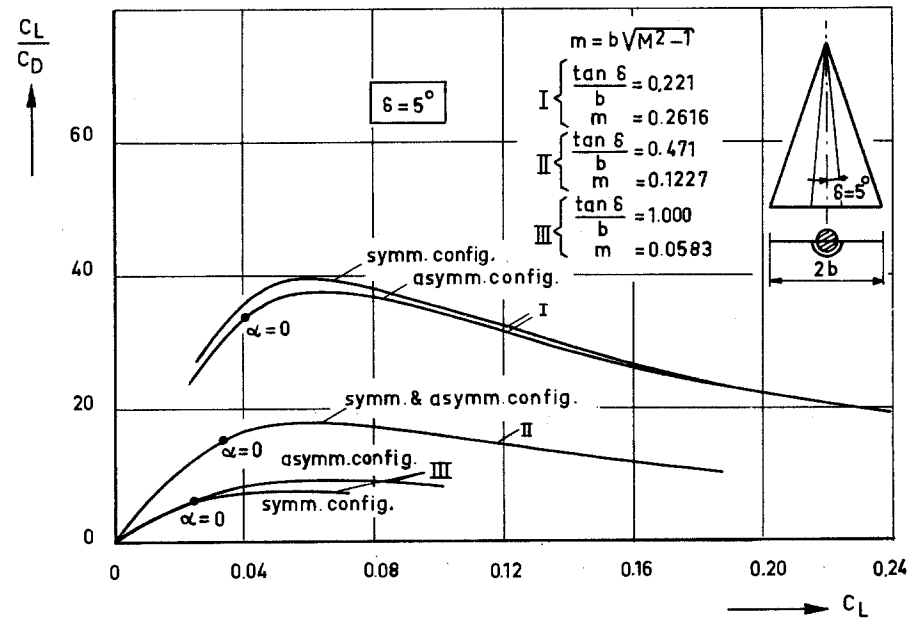

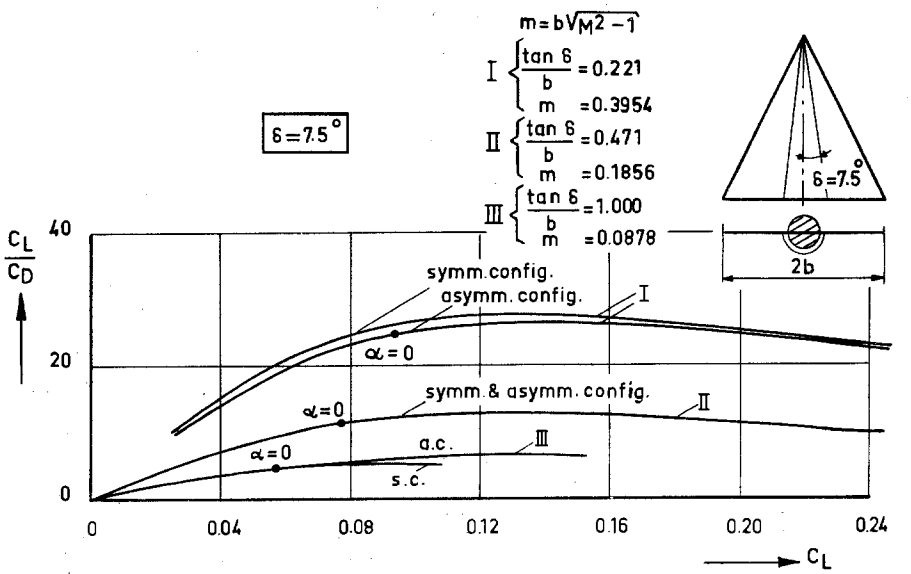

Fig. 10: $\frac{C_L}{C_D} - C_L$ for several wing-body configurations at M = 1.2

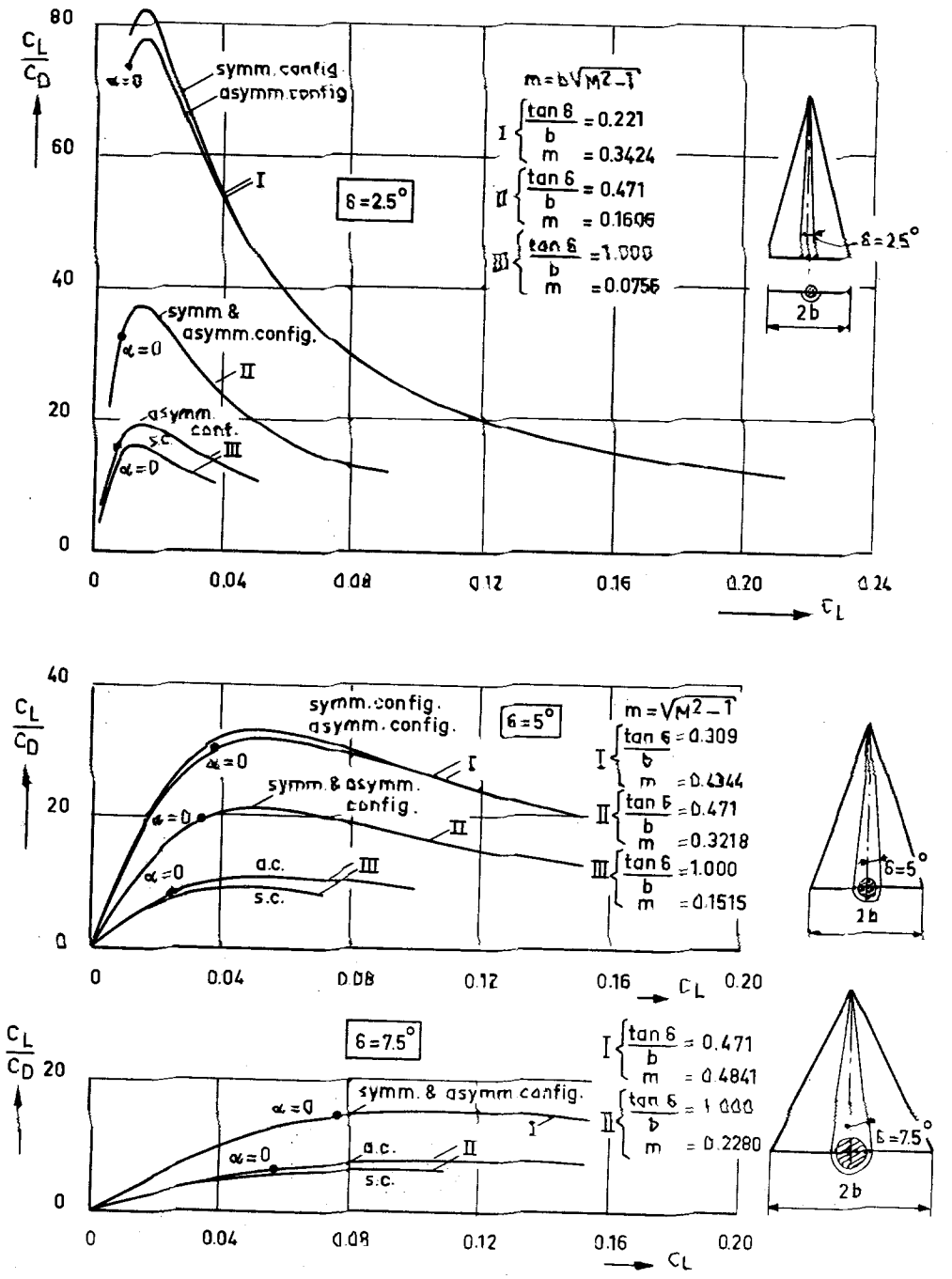

Fig. 11: $\frac{C_L}{C_D}$-C_L for several wing-body configurations at M=2.0

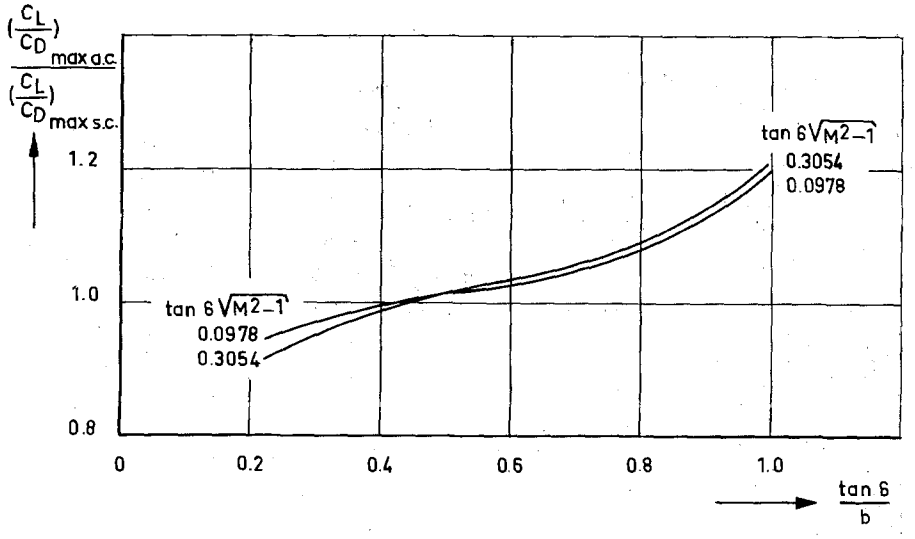

Fig. 12: Comparison between $\left(\frac{C_L}{C_D}\right)_{max}$ of the symm. and asymm. configurations

Fig. 12 shows the ratio of $C_L/C_D)_{max}$ of the asymmetrical configuration to that of the symmetrical configuration as a function of $(\tan\delta/b)$. It may be seen that the value of $(\tan\delta/b)$ of approximately 0.45 is of importance to decide which configuration provides the best $(C_L/C_D)_{max}$.

The effect of Mach number on $(C_L/C_D)_{max}$ at a constant value of δ is shown in this figure to be weak.

9. *Discussion.*

It is well-known that the numerical accuracy of the slender body theory is not very great, except possibly for small cone angles and low supersonic Mach numbers. However, other methods to achieve quantitative results for the configurations studied in this paper would be considerably more complicated. Moreover a comparison of the various configurations on the basis of slender body theory would possibly still show the trend in their relative behaviour.

In the present investigation the effect of base drag, skin friction and flow separation has been ignored. For small cone angles and equal base area the base drag might be expected to be roughly the same for the configurations studied, so that in this respect a comparative investigation would still lead to reasonable conclusions.

Since, especially for small cone angles, the wetted surface for the wing-cone configurations studied is almost equal, the effect of skin friction would probably cause primarily a uniform translation of the polar curves to higher values of C_D. The critical and optimum values do not change due to such a shift, and the drag reductions remain unchanged. The relative drag reductions will decrease however, especially for lower values of C_D, and therefore for lower values of C_L. It is obvious that the influence of skin friction on the values of C_L/C_D is very large.

Leading edge separation will certainly occur at higher angles of α. In this respect the high-wing combination is in favour on the corresponding low- and mid-wing combinations, sine the same C_L is reached at values of α.

References

1. Ferri, A., and Clarke, J.H. On the Use of Interfering Flow Fields for the Reduction of Drag at Supersonic Speeds, Journal of the Aeron. Sciences, Vol. 24, nr. 1, p. 1. January 1957.

2. Ferri, A., Clarke, J.H., and Ting, L., Favourable Interference in Lifting Systems in Supersonic Flow, Journ. of the Aeron. Sciences, Vol. 24, nr. 11, p. 791, January 1957.

3. Reyn, J.W., and Clarke, J.H. An Assessment of Body-Lift Contributions and of Linearized Theory for some Particular Wing-Body Configurations, Pibal Rep. nr. 305, Polytechnic Institute of Brooklyn, June 1956.

4. Ward, G.N. Linearized Theory of Steady High Speed Flow, Cambridge University Press, 1955.

5. Portnoy, H. The Flow Past a Delta-Wing-Half-Cone Combination with Subsonic Leading Edges, The Aeron. Quarterly, Vol. XV, p. 311, November 1964.

6. Portnoy, H. The Slender Wing with a Half Body of Revolution Mounted Beneath, To be published, 1968

7. Bannink, W.J. and Reyn, J.W. Lift and Drag Calculations on Delta Wing-Cone Configurations having Subsonic Leading Edges, Using the Slender-Body Theory (In Dutch), Report VTH-141, Technological Univ. Delft, Dep. of Aeron, Eng., January 1967.

[Received February 23, 1968]